MALAYSIAN JOURNAL OF MICROSCOPY

Journal homepage: https://malaysianjournalofmicroscopy.org

RESEARCH ARTICLE

PREPARATION AND CHARACTERIZATION OF PLA/HAp COMPOSITE FOR BIOMEDICAL APPLICATIONS

Mohamed Saiful Firdaus Hussin[1,2], Maizlinda Izwana Idris[1,*], Hasan Zuhudi Abdullah[1], Mohd Fariduddin Mukhtar[2], Mohammad Fikrey Roslan[1], Mohd Nazri Ahmad[3]

[1]*Faculty of Mechanical and Manufacturing Engineering, Universiti Tun Hussein Onn Malaysia, Parit Raja, 86400 Batu Pahat, Johor, Malaysia.*

[2]*Faculty of Mechanical Technology and Engineering, Universiti Teknikal Malaysia Melaka, Hang Tuah Jaya, 76100 Durian Tunggal, Melaka, Malaysia.*

[3]*Faculty of Industrial and Manufacturing Technology and Engineering, Universiti Teknikal Malaysia Melaka, Hang Tuah Jaya, 76100 Durian Tunggal, Melaka, Malaysia.*

Abstract. Producing scaffolds using hydroxyapatite (HAp) presents several challenges, including difficulties in controlling porosity, achieving desired mechanical properties, and addressing the brittle nature of HAp. Polylactic acid (PLA) and HAp composites with various mixing ratio were produced by an internal mixer brabender to create excellent biocompatible and biodegradable scaffolds for biomedical applications. The properties of pure PLA and PLA/HAp composite were analyzed in morphological structure, thermal stability, functional groups, and surface roughness using a scanning electron microscope (SEM), thermogravimetric analysis (TGA), Fourier transform infrared spectroscopy (FTIR), and atomic force microscopy (AFM), respectively. SEM images combined with energy dispersive spectroscopy (EDS) showed porous materials with fine grains. Pure PLA showed the presence of carbon (C) and oxygen (O) peaks while PLA/HAp composite shows the presence of additional elements which are calcium (Ca) and phosphorus (P). Meanwhile, TGA results showed the value of peak decomposition temperature decreases with the decreasing composition of PLA in the composite. The functional groups assessment showed the presence of a carbonyl group (CO) and C-H bonds for pure PLA, while the PLA/HAp composite showed the presence of additional phosphate groups. In terms of surface roughness, AFM showed increasing amounts of HAp in the PLA matrix lead to an increase in the average roughness, which can lead to better cell attachment to the composite. The results indicated that the composite with a PLA/HAp weight ratio of 70/30 accomplished more favorable properties for biomedical applications.

Keywords: Composite, hydroxyapatite, polylactic acid, morphology, surface roughness.

Article Info

Received 15 March 2025
Accepted 12 October 2025
Published 4 December 2025

***Corresponding author: izwana@uthm.edu.my**

ISSN: 1823-7010, eISSN: 2600-7444

1. INTRODUCTION

Despite remarkable progress in biomaterials and medical technologies, the development of ideal implant materials still presents considerable challenges. One of the primary concerns lies in ensuring both physical and biochemical compatibility of implants with the surrounding bone tissue. A mismatch in the mechanical and biological properties can compromise proper implant fixation, cause damage to adjacent bone, and eventually shorten implant lifespan. This problem is particularly evident with conventional metallic implants. Materials such as stainless steel, cobalt–chromium alloys, and titanium-based alloys have been widely adopted owing to their strength and durability [1]. However, these materials were originally designed for structural and industrial applications rather than biomedical purposes. Their high stiffness compared to natural bone often results in a phenomenon known as "stress shielding," where the implant bears the majority of the mechanical load. Consequently, the surrounding bone tissue experiences reduced physiological stress, which may trigger localized bone resorption and osteoporosis, thereby reducing long-term implant success.

To overcome these drawbacks, tissue engineering has emerged as a promising approach. This interdisciplinary field combines principles of cell biology, medical science, and materials engineering to design biological substitutes capable of restoring, maintaining, or enhancing tissue function. Within hard tissue regeneration, scaffolds play a central role by serving as a three-dimensional platform that mimics the extracellular matrix. An ideal scaffold should possess biocompatibility, suitable mechanical strength, interconnected porosity, and surface characteristics that promote cell adhesion, proliferation, migration, and differentiation. Designing scaffolds that meet both structural and biological requirements remains a major challenge in bone tissue [2].

Among the various biomaterials studied, hydroxyapatite (HAp, $Ca_{10}(PO_4)_6(OH)_2$) has attracted significant attention because its composition closely resembles the mineral phase of natural bone [3]. This compositional similarity contributes to its excellent bioactivity, osteoconductivity, and ability to form strong chemical bonds with native bone. For these reasons, HAp-based materials have been extensively investigated for bone repair, coatings, and scaffold fabrication. However, HAp is inherently brittle and exhibits poor mechanical strength under load-bearing conditions, which limits its use as a standalone biomaterial. To address this limitation, researchers have explored composite strategies, combining HAp with biodegradable polymers to achieve both bioactivity and improved mechanical performance.

Among polymeric candidates, polylactic acid (PLA) stands out as one of the most promising matrices. PLA is a biodegradable, biocompatible thermoplastic polymer derived from renewable resources such as corn starch and sugarcane. Its biodegradability enables gradual resorption within the body, while its mechanical strength is superior to many other biodegradable polymers. PLA has been approved for various biomedical applications, including sutures, drug delivery systems, and bone fixation devices [4]. However, pure PLA scaffolds lack intrinsic osteoinductive properties, meaning they cannot effectively stimulate bone formation on their own. This limitation has motivated the development of PLA/HAp composites, where the incorporation of HAp particles into the PLA matrix enhances bioactivity, osteoconductivity, and overall biological performance.

Various processing methods have been reported for preparing PLA/HAp composites, including solvent casting, melt blending, electrospinning, and extrusion. Among these, melt mixing using an internal mixer or twin-screw extruder offers several advantages: it ensures homogeneous dispersion of HAp particles, avoids toxic organic solvents, and yields composite pellets suitable for subsequent processing such as 3D printing. With the rapid advancement of additive manufacturing technologies, 3D printing has become an attractive tool for fabricating patient-specific scaffolds. This approach allows precise control over scaffold architecture, porosity, and mechanical properties, making PLA/HAp composites highly relevant for personalized bone tissue engineering applications.

The present study focuses on the preparation of PLA/HAp composite pellets using an internal Brabender mixer at varying HAp concentrations. The produced composites are then systematically characterized to evaluate their suitability as feedstock for 3D printing applications. Specifically, this work investigates the morphological features, thermal stability through thermogravimetric analysis, functional groups using Fourier-transform infrared spectroscopy (FTIR), and surface roughness analysis. The outcomes of this study are expected to provide fundamental insights into the structure–property relationship of PLA/HAp composites and contribute to the development of advanced biomaterials for bone tissue regeneration.

2. MATERIALS AND METHODS

HAp was extracted from *Fringescale sardinella* bones using calcination method at 900 ℃, explained in the previous study [5,6]. PLA (Emory – biomedical grade) was supplied by Saintifik Bersatu Sdn. Bhd. Pure PLA and PLA/HAp composites with 10,20, and 30 wt% of HAp were processed in a mixing chamber (internal mixer brabender) as shown in Figure 1. The pure PLA and PLA/HAp were mixed for 10 minutes at 50 rpm at 180 ℃. The mass amount of HAp gives the nomenclature of composites for instance, PLA/HAp composite with 10% HAp denoted as PLA90HAp10.

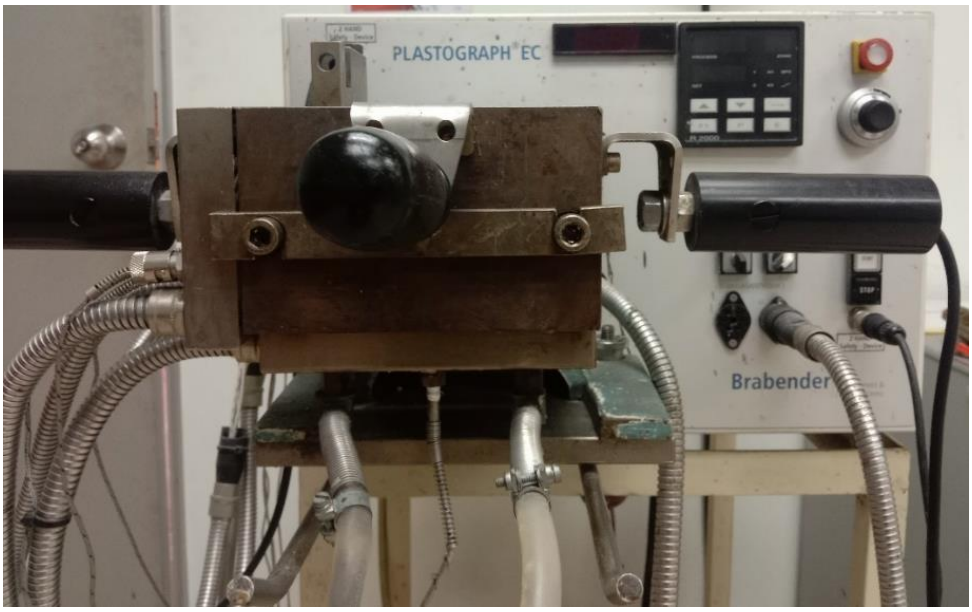

Figure 1: Internal mixer brabender

The morphological structure of pure PLA and PLA/HAp composite were observed under SEM with EDS, SU1510 (Hitachi, Japan) at 1000x magnification with 10 kV. The samples were coated with a thin layer of gold using a sputter coater to enhance imaging quality. The thermal stability and identification of decomposition stages of pure PLA and PLA/HAp was assessed by heating the samples from 30 ℃ to 700 ℃ at a rate of 10 ℃ per minute using Thermogravimetric Analysis (TGA) (Linseis, Germany). 25 mg powder was taken from the PLA and PLA/HAp samples and placed into an alumina crucible (sample cup) prior to analysis.

The functional groups of all samples were evaluated using FTIR (Perkin Elmer, USA) with universal ATR. The spectra were set in the region of 400 to 4000 cm^{-1}. The samples were characterized physically using AFM (Park System XE-100, Korea) to reveal variations in surface roughness resulting from changes in composition. AFM is used to measure and analyze surface topography of the samples at the nanometer scale, providing detailed insights into roughness and texture. The key parameter measured is the mean height variation from the central surface plane of average surface roughness. The analyses were performed under ambient conditions with calibrated piezo-scanner with a maximum xy-

range of 50 µm x 50 µm and a z scan range of 12 µm. Measurements covered randomly selected 20 µm × 20 µm surface areas.

3. RESULTS AND DISCUSSION

3.1 Morphology Analysis

The SEM images demonstrated the behaviour of PLA and HAp particles in PLA after melt-mixing process in internal mixer brabender as shown by Figure 2. The microstructure results in a material that is quite porous and contains fine grains that are related to one another.

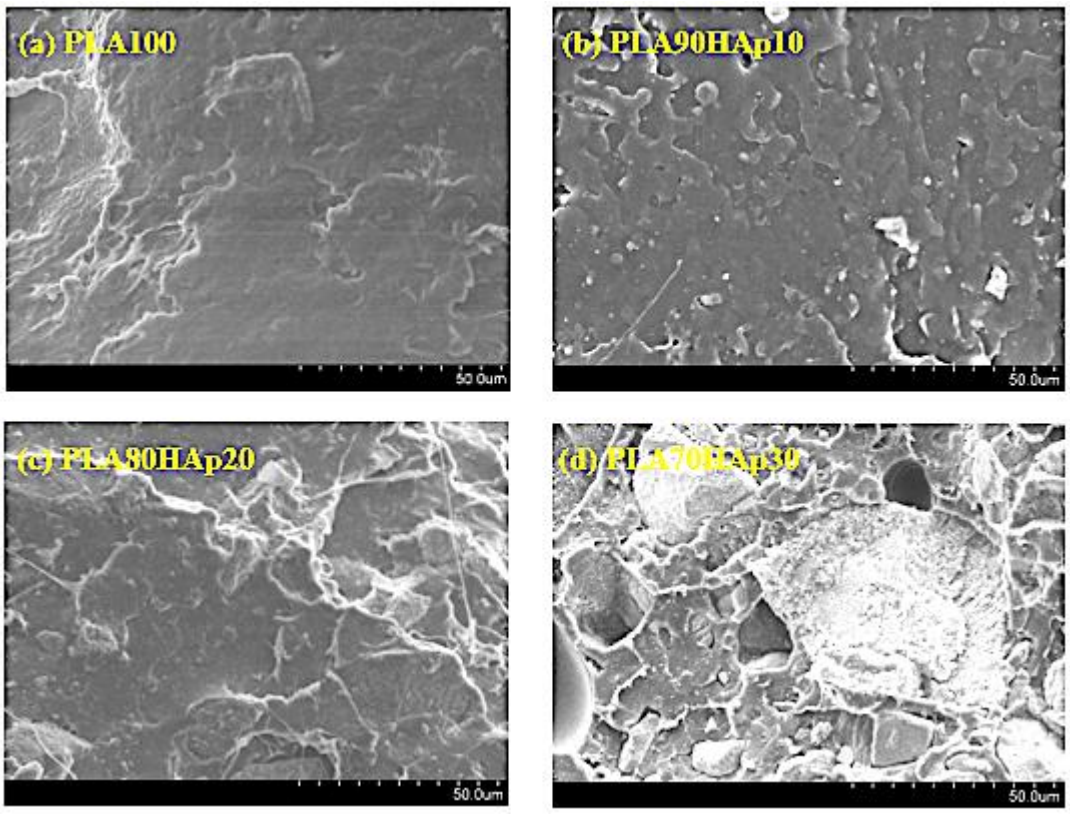

Figure 2: SEM images of (a) PLA and (b)-(d) PLA/HAp composites

Pores are essential for the development of bone tissue because they enable the movement and proliferation of osteoblast and mesenchymal cells, as well as vascularization. Pores also allow for the production of new blood vessels. A porous surface also increases the mechanical interlocking between the implant biomaterial and the native bone that surrounds it, which ultimately provides improved mechanical stability at this crucial contact [7-9].

PLA100 showed agglomerate particles represents pure PLA. PLA90HAp10 shows that HAp particle has not well-dispersed into the PLA due to lack of tendency to interact between HAp and PLA. Based on SEM image, PLA80HAp20 revealed the interfacial bonding particles microstructure between HAp and PLA. HAp and PLA has begun to incorporate with each other due to the increased of HAp weight percentage to 20% but there are a few areas that are not well-dispersed. Meanwhile, PLA70HAp30 exhibit homogenous mixture and rough surface feature of PLA/HAp composite. HAp has well-dispersed uniformly into the PLA matrix and that porosity can be detected in a clear and distinct manner.

3.2 Elemental Composition

PLA100 showed the presence of carbon (C) and oxygen (O) peaks while the mixture of PLA and HAp showed the presence of additional element; calcium (Ca) and phosphorus (P). The presence of Ca and P elements of composite samples indicated that HAp content as filler has been dispersed into the PLA as polymer matrix (Table 1). The higher HAp content added as filler in the PLA/HAp composites, the higher is the weight ratio of calcium and phosphorus [10].

Table 1: Elemental composition of PLA and PLA/HAp composites

Composite	Elements, wt%			
	C	O	Ca	P
PLA100	58.05	41.95	0	0
PLA90HAp10	54.49	39.61	1.52	4.37
PLA80HAp20	51.72	40.27	1.48	6.54
PLA70HAp30	37.38	35.75	6.33	20.54

3.3 Thermal Analysis

TGA curve will present the boundary conditions for the processing of thermoplastic materials. The decomposition temperature of each sample blend is shown by Table 2. The initial decomposition temperature means that the initial thermal stability was categorized at 10% weight loss. The value of peak decomposition temperature was proportional to the quantity of PLA present [11,12]. HAp surfaces expose Ca^{2+}, PO_4^{3-}, and OH^- groups. These ionic sites can catalyse the breaking of ester-bond in PLA when the polymer is heated. Catalytic chain breakage reduces the energy needed to start degradation, which lower the T_{ini} and T_f [13]. In addition, mineral fillers usually have higher thermal conductivity than polymer. Increased heat conduction within the sample makes local polymer regions reach decomposition temperatures faster, producing an earlier mass loss signal. The effect tends to make the onset appear earlier on TGA [14,15]. Further, the polymer chain adsorbed onto filler surfaces can be locally constrained or polarized, changing their thermochemical stability. Interfacial regions can act as initiation sites for decomposition because of altered chain mobility and local stress, which led to lower T_{ini} [16,17].

The initial and peak decomposition temperature of PLA and PLA/HAp composites were obtained by TGA curve shown in Figures 3a and 3b.

Table 2: Decomposition temperature of PLA and PLA/HAp composite

Sample Coding	Composition		Initial Decomposition Temperature, T_{ini}	Peak Decomposition Temperature, T_f
	PLA	HAp		
PLA100	100	0	314.18	369.42
PLA90HAp10	90	10	309.95	361.23
PLA80HAp20	80	20	296.69	354.16
PLA70HAp30	70	30	291.77	351.55

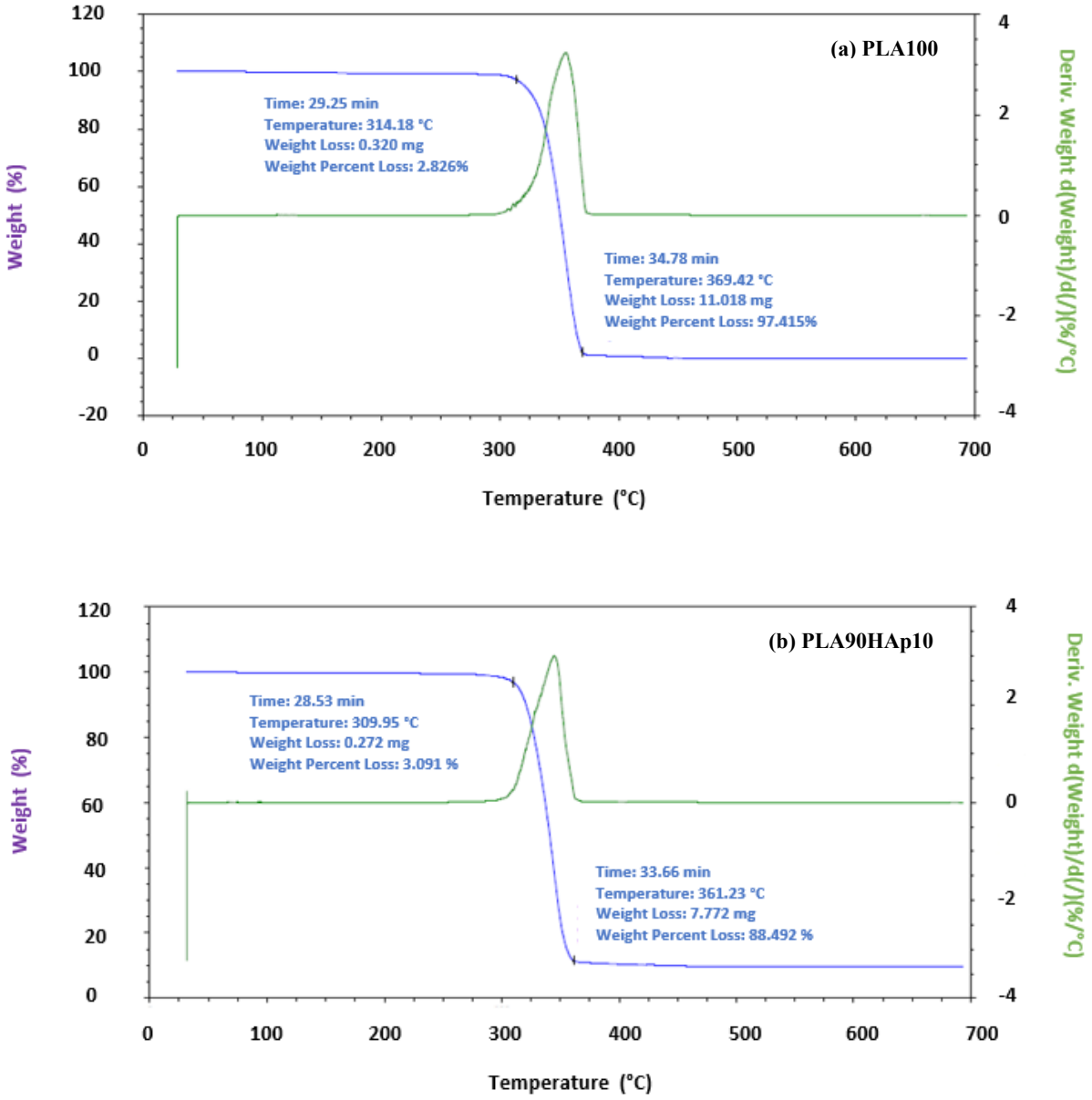

Figure 3a: TGA curves of (a) PLA and (b) PLA90HAp10 composite

TGA curve for PLA100 shows that the sample still has approximately 3 % of total weight after the peak decomposition temperature occurred. It displays strong molecular weight dependence of chain mobility particle inside PLA thus can influence the static response as well as mechanical behavior of PLA. A displays TGA curves changed significantly for all composite samples where the weight loss drops constantly. The increase in thermal stability has been attributed to the formation of strong hydrogen bonds and Van der Walls forces between the inorganic nanoparticles and the biopolymer chains during the melt-mixing process [18,19].

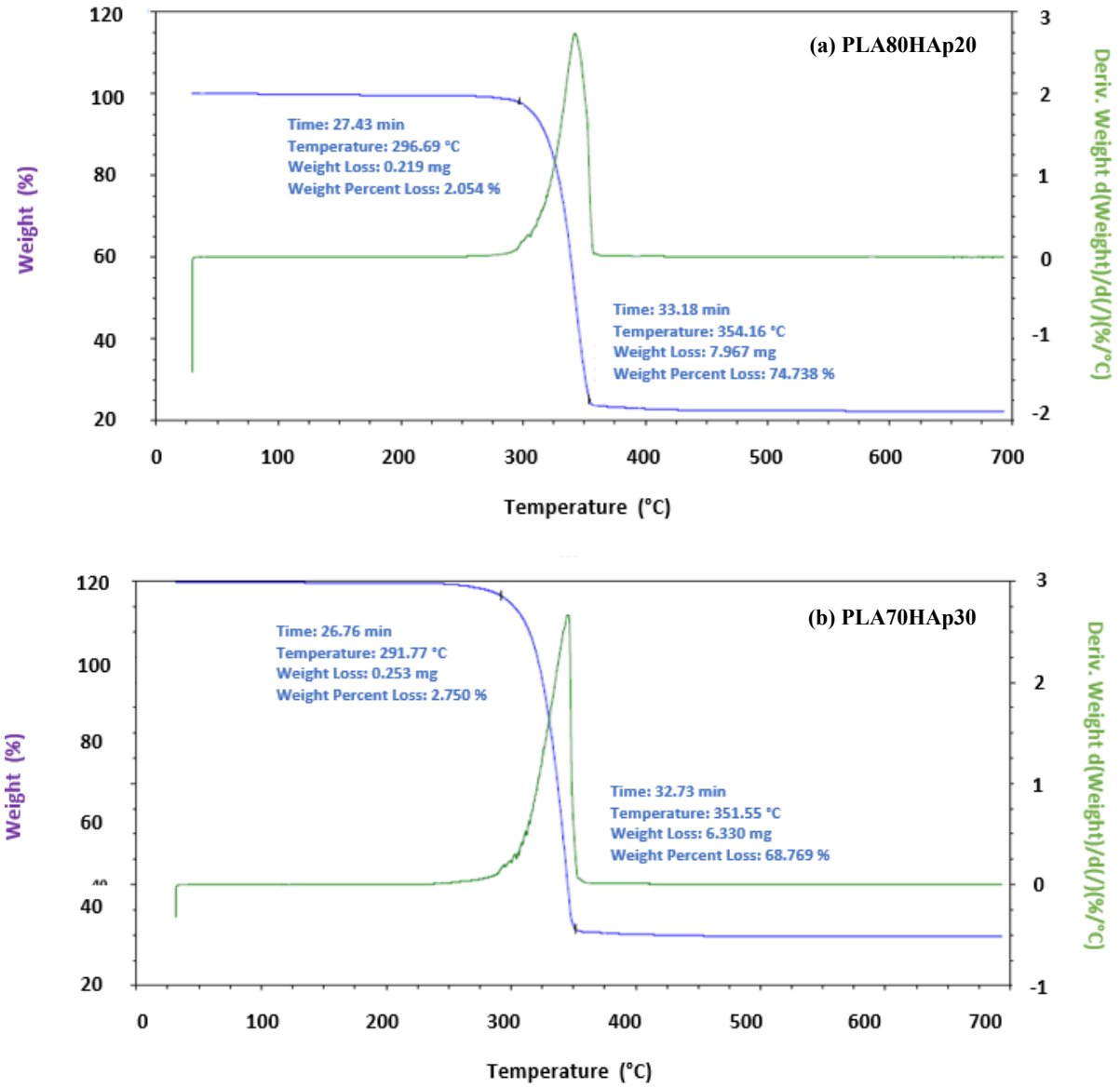

Figure 3b: TGA curves of (a) PLA80HAp20 and (b) PLA70HAp30 composites

3.4 Functional Group

Figure 4 presents the infrared absorption spectra for different compositions. The PLA100 spectrum (Figure 4(a)) shows the carbonyl group (CO) absorption band at 1748 cm^{-1}. The characteristic C-H absorption bands for pure PLA appear at 2921cm^{-1} and 2850 cm^{-1}. Additionally, the asymmetric and symmetric bending modes of the methyl group are observed between 1452 cm^{-1} to 1358 cm^{-1}. For the composites (Figure 4(b) to (d)), the stretching vibrations of the C=O (carbonyl group of the ester) are also observed at 1748 cm^{-1}. The C-H bands for pure PLA are found at 2996 cm^{-1} and 2946 cm^{-1}, corresponding to the asymmetric and symmetric C-H stretching of CH_3. A band at 3508 cm^{-1} is attributed to the hydroxyl (OH) groups of the polymers. The PO_4^{3-} bands are observed at frequencies of 1180 to 1043 cm^{-1}, 956 cm^{-1}, 808 cm^{-1} and 704 cm^{-1}. These absorption bands closely resemble the results reported by Liu et al. and Peremel et al. [20,21]. The incorporation of HAp into PLA has slightly decreases the carbonyl peak intensity (1745 cm^{-1}) and a minor shift toward lower wavenumbers is observed. This shift suggests hydrogen bonding between PLA's ester carbonyl groups and HAp's hydroxyl groups [22]. For C-O stretching, broadening and intensity increase are visible when HAp is

present. This indicates the interaction between PLA's ester C-O bonds and calcium/phosphate groups in HAp. At phosphate vibration peaks, the bands become more pronounced with higher HAp content. This confirm the successful incorporation and increasing fraction of HAp in the composite [23]. With higher HAp content, PLA peaks become weaker relative to phosphate peaks, showing increasing mineral dominance. Hydrogen bonding occurs between carbonyl group and hydroxyl group. These interactions improve interfacial adhesion between PLA and HAp, which is crucial for mechanical reinforcement and biocompatibility. However, excessive HAp loading may cause peak broadening and reduced PLA band intensity, suggesting agglomeration or poor dispersion at high loadings [24].

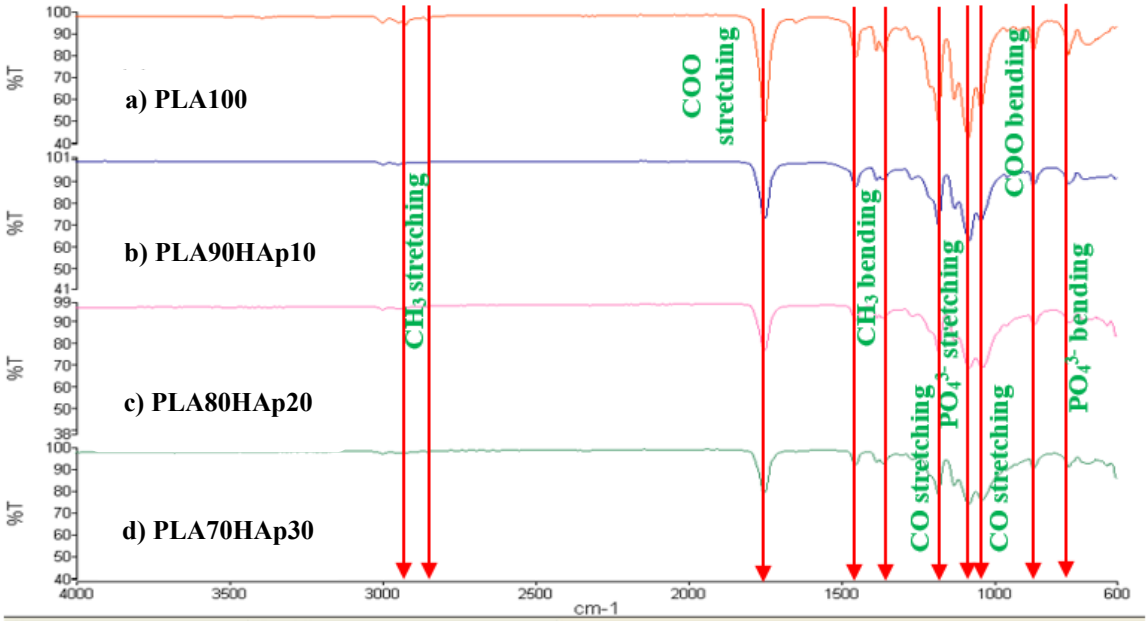

Figure 4: FTIR spectra of (a) PLA and (b-d) PLA/HAp composites

3.5 Surface Roughness

Figure 5 illustrates the 3D morphology of the surfaces of PLA and PLA/HAp composites.

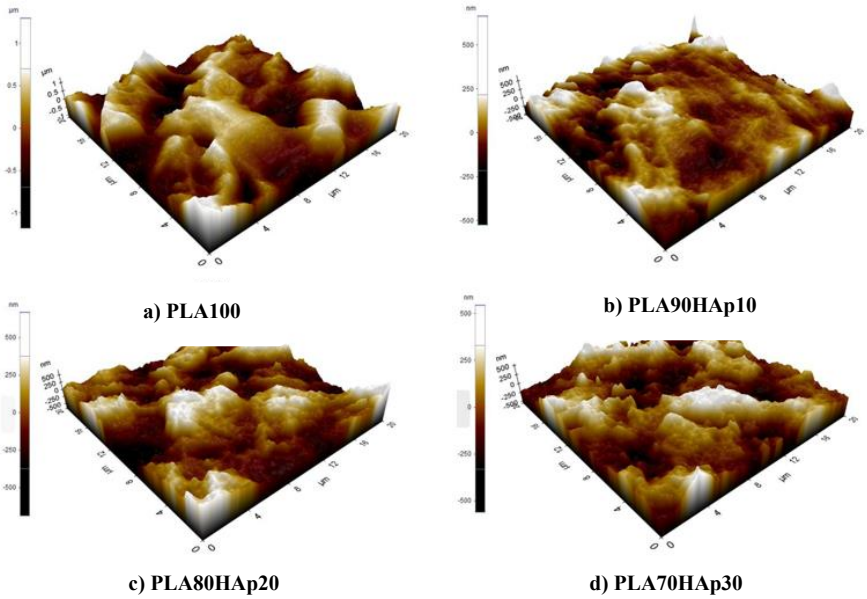

Figure 5: AFM images of (a) PLA and (b-d) PLA/HAp composites

The pure PLA sample exhibits a surface topography with areas of high roughness areas as well as smoother region, with an average roughness of 7.43 nm. The PLA90HAp10 composite film displays an increase in the average roughness, measuring approximately 11.03 nm. This increase is attributed to the formation of HAp aggregates on the active surface of the membrane, showing similar patterns to those observed in the SEM images. The surface of the composite membrane becomes more organized due to improved HAp dispersion, with average roughness values rising to 14.68 nm and 21.82 nm, for PLA80HAp20 and PLA70HAp30, respectively. These unique properties of the composites will enhance cell attachment and osteogenic differentiation [25,26].

4. CONCLUSIONS

Developing new materials tailored to the unique requirement of hard tissue engineering applications presents a significant challenge. PLA100 exhibit a relatively smooth and uniform fracture surface. The addition of HAp showed rougher surface of the composites with visible particle distribution. At higher loading (30 wt%), HAp agglomeration and void formation were observed, suggesting reduced interfacial bonding. In TGA, increasing HAp content progressively decreased both T_{ini} and T_f. The reduction in thermal stability is attributed to the catalytic effect of HAp surface groups and increased interfacial sites, which accelerate chain reaction. FTIR results show a slight shift and reduction in the intensity of the PLA carbonyl peak upon incorporation of HAp, which suggest hydrogen bonding between the C=O groups of PLA and the hydroxyl groups of HAp. From AFM images, the gradual increase in nanoscale roughness enhances surface activity, which is advantageous for cell adhesion, proliferation, and osteogenic differentiation, which are the key requirement for biomedical scaffolds. Therefore, the material is suitable for 3D printing of biomedical scaffolds, successfully meeting the study's objective of developing a bioactive, printable composite for bone tissue engineering applications.

Acknowledgements

Authors would like to thank Universiti Tun Hussein Onn Malaysia (UTHM) through the funding via Tier 1 grant Q495.

Author Contributions

All authors contributed toward data analysis, drafting and critically revising the paper and agree to be accountable for all aspects of the work.

Disclosure of Conflict of Interest

The authors have no disclosures to declare

Compliance with Ethical Standards

The work is compliant with ethical standards

References

[1] Kim, T., See, C. W., Li, X. & Zhu, D. (2020). Orthopedic implants and devices for bone fractures and defects: past, present and perspective. *Engineered Regeneration,* 1, 6-18.

[2] Sriprapha, P., Chokethawai, K., Randorn, C., Chandet, N., Thongkorn, K., Saenkam, K., Boontakam, W. & Rujijanagul, G. (2024). Induced porous structure with a slight change in mechanical properties of hydroxyapatite-based nanocomposites synthesized from waste bovine bone and their bioactivity. *Materials Today Sustainability,* 26, 100710.

[3] Abirafin, F. B., Musa, Z. & Abirafin, J. K. (2023). Mechanical processing of hydroxyapatite through sintering and multi-objective optimization technique for biomedical application. *Materials Research Society Advances,* 8(9), 532-537.

[4] Hussin, M. S. F., Abdullah, H. Z., Idris, M. I. & Wahab, M. A. A. (2022). Extraction of natural hydroxyapatite for biomedical applications—a review. *Heliyon,* 8(8), e10356.

[5] Hussin, M. S. F., Idris, M. I., Abdullah, H. Z., Azeem, W. & Ghazali, I. (2023). Characterization and in vitro evaluation of hydroxyapatite from *Fringescale sardinella* bones for biomedical applications. *Journal of Saudi Chemical Society,* 27(5), 101721.

[6] Hussin, M. S. F., Idris, M. I., Abdullah, H. Z. & Sultan, A. A. (2024). Synthesis and characterisation of hydroxyapatite from Fringescale sardinella for biomedical applications. *AIP Conference Proceedings,* 2925(1), 020045.

[7] Bandyopadhyay, A., Mitra, I., Goodman, S. B., Kumar, M. & Bose, S. (2023). Improving biocompatibility for next generation of metallic implants. *Progress in Materials Science,* 133, 101053.

[8] Liu, X., Zhou, C., Xie, Q., Xia, L., Liu, L., Bao, W., Lin, H., Xiong, X., Zhang, H., Zheng, Z., Zhao, J. & Liang, W. (2024). Recent advances in layer-by-layer assembly scaffolds for co-delivery of bioactive molecules for bone regeneration: an updated review. *Journal of Translational Medicine*, 22, 1001.

[9] Ghorbani, F., Sahranavard, M., Nejad, Z. M., Li, D., Zamanian, A. & Yu, B. (2020). Surface functionalization of three dimensional-printed polycaprolactone-bioactive glass scaffolds by grafting GelMA under UV irradiation. *Frontiers in Materials,* 7, 528590.

[10] Pradid, J., Keawwatana, W., Boonyang, U. & Tangbunsuk, S. (2017). Biological properties and enzymatic degradation studies of clindamycin-loaded PLA/HAp microsphere prepared from crocodile bones. *Polymer Bulletin*, 74(12), 5181-5194.

[11] Bauer, L., Rogina, A., Ivankovic, M. & Ivankovic, H. (2023). Medical-grade poly(lactic acid)/hydroxyapatite composite films: thermal and in vitro degradation properties. *Polymers,* 15(6), 1512.

[12] Pandele, A. M., Constantinescu, A., Radu, I. C., Miculescu, F., Voicu, S. I. & Ciocan, L. T. (2020). Synthesis and characterization of PLA-micro-structured hydroxyapatite composite films. *Materials,* 13(2), 274.

[13] Teixiera, S., Eblagon, K. M., Miranda, F., Pereira, M. F. R., Figueiredo, J. L. (2021). Towards controlled degradation of poly(lactic) acid in technical applications. *Journal of Carbon Research*, 7(2), 42.

[14] Melnyk, L. (2024). Influence of mineral filler on the thermal conductivity of polymer composites. *Technology Audit and Production Reserves*, 6(3), 6-11.

[15] Rosel, U. & Drummer, D. (2025). Correlation of the thermal conductivity and mechanical properties in hybrid filler systems of thermosets. *Polymers*, 17(14), 1924.

[16] Nakatai, A. I., Mohler, C. E. & Hughes, S. (2021). Chain conformation of polymers adsorbed to clay particles: effects of charge and concentration. *Soft Matter*, 17(28), 6848-6862.

[17] Raza, A., Mushtaq, A. & Saleem, A. (2024). Effect of modified waste bio-filler for sustainable reinforced polymer composite for a circular economy. *Iranian Journal of Chemistry and Chemical Engineering*, 43(9), 3498-3511.

[18] Kervran, M., Vagner, C., Cochez, M., Poncot, M., Saeb, M. R. & Vahabi, H. (2022). Thermal degradation of polylactic acid (PLA)/polyhydroxybutyrate (PHB) blends: a systematic review. *Polymer Degradation and Stability*, 201, 109995.

[19] Ng, K. M. P., Tan, I. S., Foo, H. C. Y., Lau, J. S. Y., Lam, M. K. & Wong, M. K. (2024). Durable polylactic acid bionanocomposites with biomass-derived nanocellulose additives: recent advances in production. *Journal of the Taiwan Institute of Chemical Engineers*, 177, 105774.

[20] Liu, S., Zheng, Y., Liu, R. & Tian, C. (2020). Preparation and characterization of a novel polylactic acid/hydroxyapatite composite scaffold with biomimetic micro-nanofibrous porous structure. *Journal of Materials Science: Materials in Medicine,* 31(8), 74.

[21] Peremel, S., Jaafar, C. N. A., Zainol, I., Ariffin, M. K. A. & Chen, S. (2023). The properties of poly(lactic acid) (PLA)/ hydroxyapatite (FsHAP) composite prepared through solvent casting techniques. *Malaysian Journal of Microscopy,* 19(1), 43-54.

[22] Custodio, C. L., Bronola, P. J. M., Cayabyab, S. R., Lagura, V. U., Celorico, J. R. & Basilia, B. A. (2021). Powder Loading Effects on the Physicochemical and Mechanical Properties of 3D Printed Poly Lactic Acid/Hydroxyapatite Biocomposites. *International Journal of Bioprinting*, 7(1), 112–122.

[23] Ricardo, P. A., Eric, M. R., Gabriel, L., Jose, R. A. & Rodrigo, V. (2022). Improving the mechanical resistance of hydroxyapatite/chitosan composite materials made of nanofibers with crystalline preferential orientation. *Materials*, 15(13), 4718.

[24] Chandra, P., Venkatarayappa, R., Chandrashekar, S.D., Raveendra, K., Bhaskararao, A.P., Bheemappa, S., Goudar, D.M., Kurhatti, R.V., Raju, K., Pinto, D.G. (2025). Enhancing the interfacial adhesion and mechanical strength of pultruded ecr-glass fiber composites with nanofiller-infused epoxy resin. *Journal of Composites Science,* 9(7), 321.

[25] Sitthisang, S., Hou, X., Treetong, A., Xu, X., Liu, W., He, C., Sae-Ueng, U. & Yodmuang, S. (2024). Nanomechanical mapping of PLA hydroxyapatite composite scaffolds links surface homogeneity to stem cell differentiation. *Scientific Reports,* 14(1), 21097.

[26] Odabas, E., Ozturk, O. & Akarsu, E. (2024). Modulation of mechanical and thermal properties of poly(lactic acid)/hydroxyapatite composites by interface crosslinking. *Polymer Composites,* 45(18), 17280-17293.